

An asymmetric supercapacitor using RuO₂/TiO₂ nanotube composite and activated carbon electrodes

Yong-Gang Wang, Zi-Dong Wang, Yong-Yao Xia*

Chemistry Department and Shanghai Key Laboratory of Molecular Catalysis and Innovative Materials, Fudan University, Shanghai 200433, China

Received 18 January 2005; received in revised form 21 March 2005; accepted 26 March 2005

Available online 26 April 2005

Abstract

We reported an asymmetric supercapacitor technology where RuO₂/TiO₂ nanotube composite was used as positive electrode and the activated carbon as negative electrode in 1 mol/L KOH electrolyte solution. The electrochemical capacitance performance of the asymmetric supercapacitor was tested by cyclic voltammetry, electrochemical impedance spectroscopy and galvanostatic charge-discharge tests. The results show that the asymmetric supercapacitor has electrochemical capacitance performance within potential range 0–1.4 V. A power density 1207 W/kg was obtained with an energy density of 5.7 W h/kg at a charge-discharge current density of 120 mA/cm². The supercapacitor also exhibits a good cycling performance and keep 90% of initial capacity over 1000 cycles.

© 2005 Elsevier Ltd. All rights reserved.

Keywords: RuO₂/TiO₂ nanotube; Active carbon; Asymmetric supercapacitor

1. Introduction

In recent years, supercapacitors are attracting great attention due to their high capacitance and potential applications in electronic devices. They can be coupled with batteries to provide pulses of peak power during acceleration and on uphill gradients. The hybrid system is stimulating the development of high performance electronic devices [1–3]. On the basis of electrode materials used and the charge storage mechanisms, electrochemical supercapacitors are classified as: (a) electrochemical double-layer capacitors (EDLCs) which employ carbon or other similar materials as blocking electrodes [4,5], and (b) redox supercapacitors in which electroactive materials such as insertion type compounds (e.g. RuO₂, NiO, etc.) or conducting polymers are employed as electrodes [6–9]. Among these materials, hydrous ruthenium oxide has been recognized as one of the most promising candidates for its good electrochemical capacitance performance and high specific capacitance. However, hydrous ruthenium oxide is very

expensive, many efforts are thereby made to replace ruthenium oxide with other transition metal oxides as electrodes in electrochemical capacitors or reduce the amount of ruthenium in the fabrication of supercapacitor.

Recently, the asymmetric supercapacitor that was regarded as the new trend in electrochemical supercapacitors has been reported greatly. The new type hybrid asymmetric supercapacitor are different from either the EDLCs or the conventional batteries. For such type capacitors, one electrode stores charge through a reversible nonfaradaic process of ionic movement on the surface of an activated carbon or the hole of a nano-pore carbon material, and another electrode is to utilize a reversible faradic reaction of redox reaction of metal oxides. [10–14]. It is possible to obtain the high working voltage of the supercapacitors by choosing a proper electrode material. Both increase of the working voltage and high energy density of the metal oxide electrode result in a significant increase of the overall energy density of the capacitors. Very recently, one author of this paper has reported that the three-dimensional nanotubes network of TiO₂ nanotubes can increase greatly the utilization of RuO₂ or NiO [15,16], and the capacitance profile of the symmetric capacitors using

* Corresponding author. Tel.: +86 21 55664177; fax: +86 21 55664177.
E-mail address: yyxia@fudan.edu.cn (Y.-Y. Xia).

of RuO₂/TiO₂ nanotubes as both positive and negative electrodes were investigated. In this study, we presented an hybrid asymmetric supercapacitor based on RuO₂/TiO₂ nanotube positive electrode combined with an activated carbon (AC) negative electrode in 1 mol/L KOH electrolyte solution. The electrochemical capacitance performance of the asymmetric supercapacitor was investigated by cyclic voltammetry (CV), electrochemical impedance spectroscopy (EIS) and galvanostatic charge–discharge tests.

2. Experimental

2.1. Preparation of electrode materials

TiO₂ nanotubes was synthesized according to the reference [15–17] (TiO₂ used in our experiment is Anatase and

purchased from Aldrich). RuO₂/TiO₂ nanotube composites were prepared by loading of RuO₂·xH₂O on TiO₂ nanotubes in an alkaline medium. The TiO₂ nanotubes were immersed in an aqueous bath containing RuCl₃·nH₂O (Aldrich) and alcohol (99.8%, ZhengXin Chemical Factory, Shanghai, China), and then 0.1 mol/L KOH was dropped into the bath with stirring until the pH of the aqueous reached to 7. The black product of the reaction was filtered and washed repeatedly with distilled water. The resulting product was dried at 105 °C. The composite with 10 wt.% RuO₂·xH₂O loaded on TiO₂ nanotubes were obtained. The morphologies of resulting composites were characterized by scanning electron microscopy (SEM) in a Philips XL-60 scanning microscope and Japan Electron tunneling electron microscopy (TEM, Jeol JEM-2010). Activated carbon with a specific area of 1500 cm²/g was used as received without further treatment.

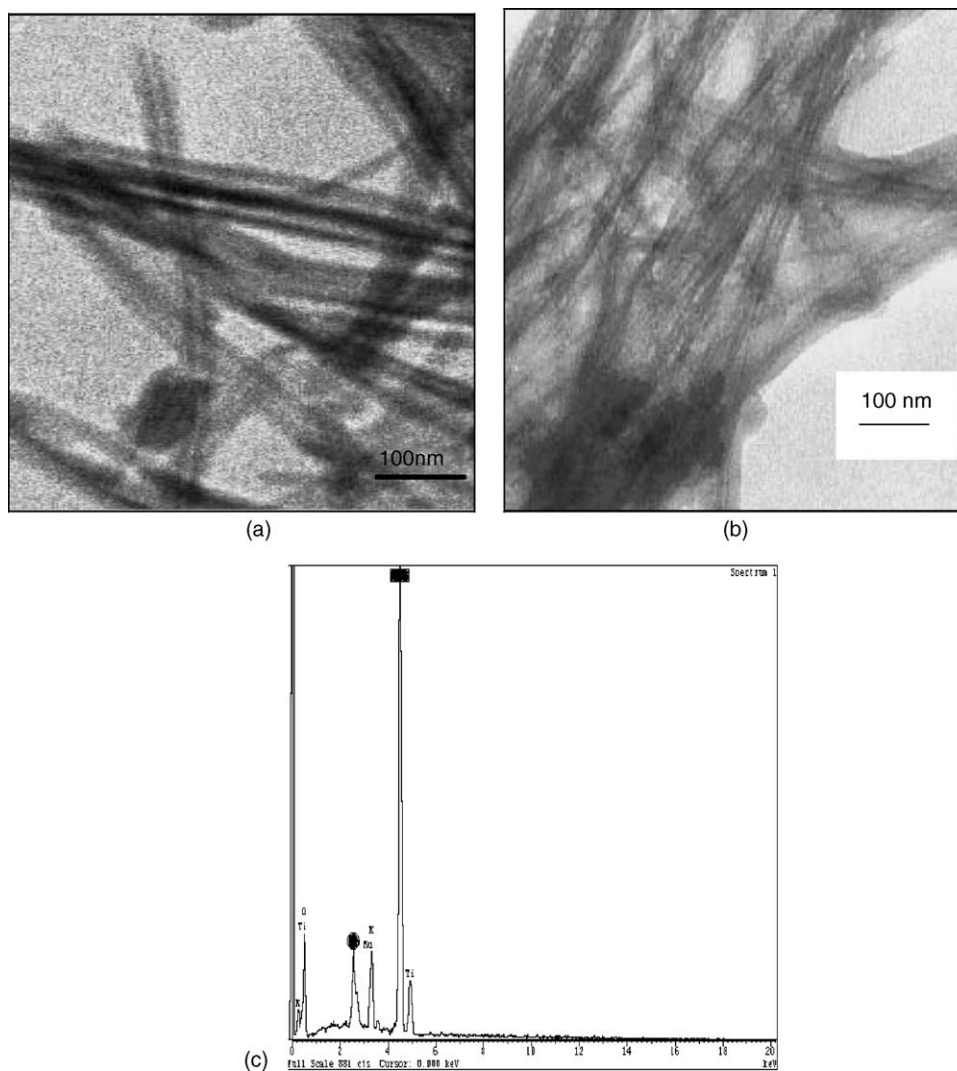


Fig. 1. TEM images of TiO₂ nanotubes and RuO₂/TiO₂ nanotube composite: (a) TiO₂ nanotubes and (b) RuO₂/TiO₂ nanotube composite. (c) EDAX pattern of RuO₂/TiO₂ nanotube composite. (●) Ru; (■) Ti.

2.2. Electrochemical tests

The electrode of RuO₂/TiO₂ nanotube composites was prepared according to the following steps. The mixture containing 80 wt.% RuO₂/TiO₂ nanotube composites and 15 wt.% acetylene black (AB) and 5 wt.% polytetrafluoroethylene (PTFE) was well mixed, and then was pressed onto nickel grid (1.2×10^7 Pa) that serves as a current collector (area is 1 cm²). The AC electrode was prepared by the same method as the positive electrode described above, it consisted of 80 wt.% AC, 15 wt.% AB and 5 wt.% PTFE. The typical mass load of positive electrode material (RuO₂/TiO₂ nanotube composites) is 40 mg and the mass load of negative electrode material (AC) is 30 mg. The electrolyte was 1 M KOH solution. Capacitor were usually cycled between the voltage of 0 and 1.4 V; the charge and discharge rates were 15, 30, 60 and 120 mA/cm², respectively.

The electrochemical behavior of the resulting compound was also characterized by cyclic voltammetry (CV) and galvanostatic charge–discharge test. The experiments were carried out in a three-electrode glass cell. Platinum foil was used as a counter electrode, and Hg/HgO as the reference electrode. CV experiment measurement and EIS measurements were performed using a Solartron Instrument Model 1287 electrochemical interface and 1255B frequency response analyzer controlled by a computer. The frequency limits were typically set between 10⁵ and 10⁻² Hz. The AC oscillation was 10 mV. The data were analyzed by Zplot software.

3. Results and discussion

3.1. The characters of TiO₂ and RuO₂/TiO₂ nanotube composite

The TEM image of TiO₂ nanotubes are shown in Fig. 1a. As seen in Fig. 1a, numerous fiber-like TiO₂ nanotubes were grown, and the hollow nature of the nanotubes is clearly visible in the TEM image. These nanotubes have an outer diameter between 20 and 30 nm and inside diameter between 10 and 15 nm. It's length is about 1 μm. Fig. 1b is the TEM image of RuO₂/TiO₂ nanotube composite, and Fig. 1c is the energy dispersive X-ray analysis (EDAX) pattern of RuO₂/TiO₂ nanotube composite. The peak around 2.50 kV shows the presence of ruthenium, it suggests that some RuO₂ was loaded on TiO₂ nanotubes.

3.2. Electrochemical tests

3.2.1. The electrochemical characters of AC and RuO₂/TiO₂ nanotube composite

Fig. 2 shows typical CV curves of RuO₂/TiO₂ nanotube composite within a potential window of -0.4 to 0.4 V (versus Hg/HgO) and AC within a potential window of -1 to 0 V (versus Hg/HgO) at a scan rate of 5 mV/s. The CV curve of AC has a rectangular shape. It is well-known that the capac-

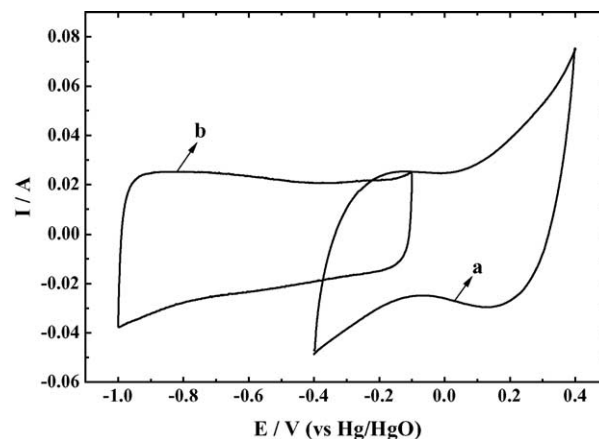


Fig. 2. CV curves of RuO₂/TiO₂ nanotube composite and AC at a scan rate of 5 mV/s: (a) RuO₂/TiO₂ nanotube composite and (b) AC.

itance of AC is based on the adsorbed charges on the surface of the electrode surface. The adsorbed charges on the electrode surface increase linearly with increasing potential. For this reason, the current intensity of AC shown in CV curve is potential independent. In other words, the current intensity of AC electrode is almost constant despite of the change of potential. However, CV curve of RuO₂ is different from that of AC, which is due to a faradic reaction of RuO₂, shown as follows:



It is not surprising that the RuO₂/TiO₂ nanotube composite show a CV shape similar to that of RuO₂, because the TiO₂ nanotubes was just used as a support to increase the utilization of RuO₂. In other words, the capacitance of RuO₂/TiO₂ nanotube composite contributed lonely from the pseudocapacitive nature of RuO₂ loading on TiO₂ support because TiO₂ nanotubes have no pseudocapacitance, which has been reported in my previous work [15].

The typical galvanostatic charge–discharge curves of RuO₂/TiO₂ nanotube composite within a potential window of -0.2 to 0.4 V (versus Hg/HgO) and AC within a potential window of -1 to 0 V (versus Hg/HgO) are shown in Fig. 3. The charge–discharge curve of AC (curve b in Fig. 3) shows a linear variation of voltage, which is due to linear correlation between the adsorbed charge on the electrode surface and its applied potential, indicating the potential independent nature of the non-faradaic process. However, a linear variation of voltage was not observed for the RuO₂/TiO₂ nanotube composite, the slope of charge curve or discharge curve changed clearly when the redox reaction occurred (curve a in Fig. 3). This is attributed to the potential dependent nature of faradic redox reaction. From the results of Fig. 3, the estimated capacity of AC is of 90 F/g in the potential window -0.2 to -1 V versus Hg/HgO, and 120 F/g of RuO₂/TiO₂ nanotube composite within the potential window -0.2 to 0.4 V. By comparing the delivered capacity, the optimal positive/negative mass ratio was set around 4:3.

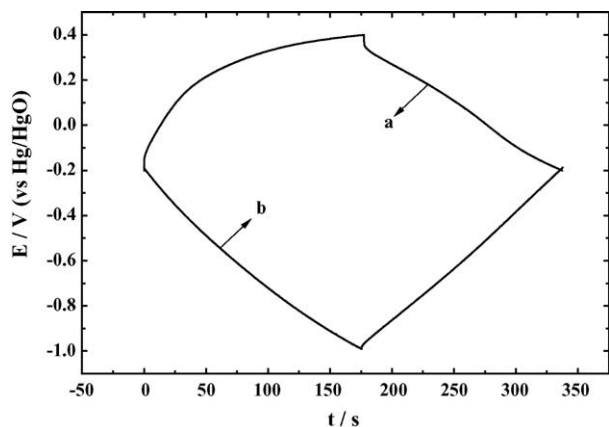


Fig. 3. Charge–discharge curves of RuO₂/TiO₂ nanotube composite and AC at a current density of 15 mA/cm²: (a) RuO₂/TiO₂ nanotube composite and (b) AC.

3.2.2. The electrochemical character of the asymmetric supercapacitor

Fig. 4 is the cyclic voltammetry response of the asymmetric supercapacitor at a scan rate of 5 mV/s in the potential range from 0 to 1.4 V. As shown in Fig. 4, the rectangle shape of CV curve suggests that the asymmetric supercapacitor has electrochemical capacitance performance within the potential range (0–1.4 V).

The electrochemical impedance measurements (at applied potential of 0.2, 0.4, 0.8 and 1.2 V; the frequency range is 10⁵ to 10⁻² Hz) were carried out and typical plots are shown in Fig. 5. Two distinct regions which are dependent on the frequency range are shown in Fig. 5a, b, c and d. From the point intersecting with the real axis in the range of high frequency, the internal resistances R_i of the supercapacitor is about 1.5 Ω. In the high frequency region, the semi-circle was not observed and the slopes of these impedance plots are low. In the low frequency region, the slopes of impedance of the asymmetric supercapacitor at different applied potential increase clearly, which indicates that the asymmetric superca-

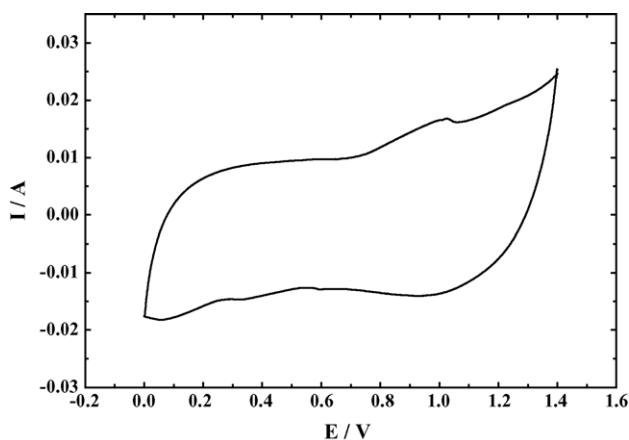


Fig. 4. CV curve of the asymmetric supercapacitor based on RuO₂/TiO₂ nanotube composite and AC at a scan rate of 5 mV/s.

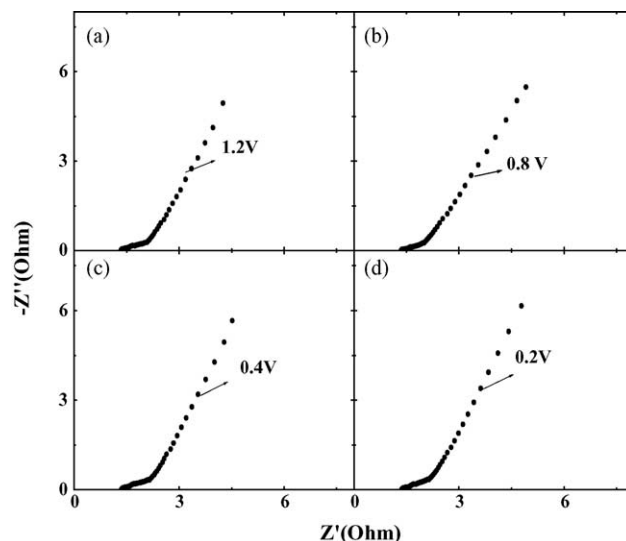


Fig. 5. EIS plots of the asymmetric supercapacitor at different applied potentials.

pacitor has electrochemical capacitance performance at these applied potentials.

The specific capacitance of the asymmetric capacitor at different applied potential can be evaluated from impedance test according to the following equations respectively:

$$C_m = \frac{C}{m} = \frac{1}{m \times (j\omega Z'')} \quad (2)$$

where C_m is the specific capacitance of the asymmetric capacitor; $j = -1$; $\omega = 2\pi f$; f is the frequency (10⁻² Hz); Z'' is the imaginary part of the impedance test; m is the mass of active materials in this capacitor (include positive and negative electrode).

The data shown in Table 1 indicate that the asymmetric capacitor has electrochemical performance at potential 0.2, 0.4, 0.8 and 1.2 V. This result is consistent with the result of CV test.

Fig. 6 shows the galvanostatic charge–discharge curves of the asymmetric supercapacitor between 0 and 1.4 V at different current densities. The specific capacitance of the supercapacitor (C_m) was calculated as follows:

$$C_m = \frac{C}{m} = \frac{I \times \Delta t_d}{\Delta V \times m} \quad (3)$$

where I is the current of charge–discharge, Δt_d is the time of discharge. ΔV is the potential range (1.4 V). The m is the mass of active materials in the asymmetric supercapacitor (include positive and negative electrode).

Table 1

The specific capacitances of the asymmetric capacitor at different applied potentials evaluated from EIS tests

Capacitance at 1.2 V (F/g)	Capacitance at 0.8 V (F/g)	Capacitance at 0.4 V (F/g)	Capacitance at 0.2 V (F/g)
46	41	40	36

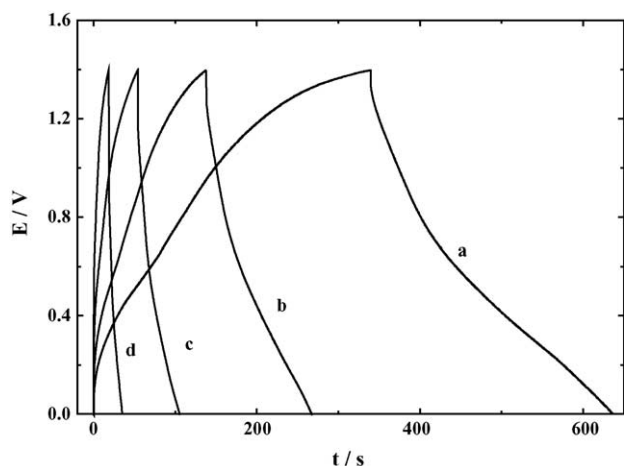


Fig. 6. Typical charge–discharge curves of the asymmetric supercapacitor at different current densities: (a) 15; (b) 30; (c) 60 and (d) 120 mA/cm².

The specific capacitances of the supercapacitor at current densities of 15, 30, 60 and 120 mA/cm² were 46, 40, 32 and 21 F/g, respectively. In reference [15], we have reported that the specific capacitance of symmetrical supercapacitor based on RuO₂/TiO₂ nanotube composite was 50 F/g within a potential range of 0–0.8 V. In summary, there are no big capacitance difference between the asymmetrical supercapacitor and symmetrical supercapacitor, but the asymmetrical supercapacitor shows a higher working voltage.

The energy density (E) of the a supercapacitor can be calculated by using the following equation:

$$E = \int V dq$$

$$C = \frac{q}{V} \quad (4)$$

$$E = C \int V dv = \frac{1}{2} C (\Delta V)^2$$

where C is the capacitance of the capacitor, ΔV are the operating potential window (1.4 V). The m is the amount of active materials in the supercapacitor (include positive and negative electrode).

The specific power density (P) of the supercapacitor can be calculated according to the following equation:

$$P = \frac{I \Delta V}{2m} \quad (5)$$

where I is the current of charge–discharge. ΔV is the potential range of a supercapacitor. The m is the mass of active materials in the asymmetric supercapacitor (include positive and negative electrode).

In order to emphasize the advantage of asymmetric supercapacitor based on RuO₂/TiO₂ nanotube composite and AC, we compared the energy density and power density of the asymmetric supercapacitor with that of symmetrical supercapacitor based on RuO₂/TiO₂ nanotube composite reported in my previous work, and the results are shown in Fig. 7. As

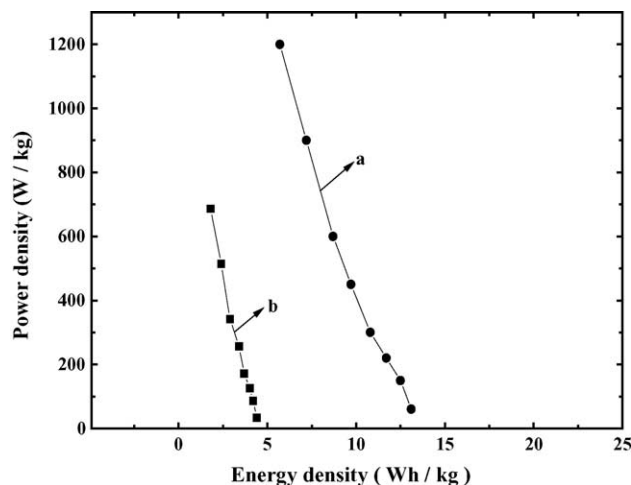


Fig. 7. Ragone plot relating power density to achievable energy density of the supercapacitor: (a) asymmetric supercapacitor based on RuO₂/TiO₂ nanotube composite and AC, (b) symmetrical supercapacitor based on RuO₂/TiO₂ nanotube composite.

shown in Fig. 7, the energy density of both supercapacitors reduced clearly with the increase in the power density. However, the energy density and power density of the symmetric supercapacitor based on RuO₂/TiO₂ nanotube composite and AC was greater than that of symmetrical supercapacitor based on RuO₂/TiO₂ nanotube composite. This can be explained by that the energy density and power density of the supercapacitor are critically dependent on both the specific energy of electrode and the working voltage as described in the Eqs. (4) and (5) [18]. Moreover, combination of AC with RuO₂/TiO₂ nanotube composite may reduce greatly the mass loading of RuO₂ compared with a symmetrical supercapacitor using both electrode of RuO₂/TiO₂ nanotube composite, but delivers a higher energy density and power density.

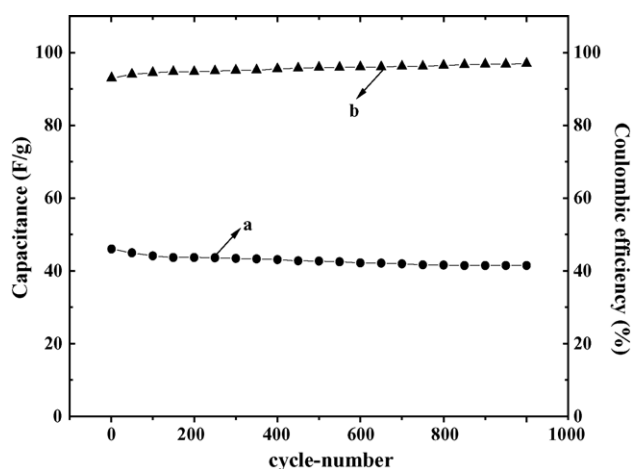


Fig. 8. Cycle charge–discharge test of the asymmetric supercapacitor at a current density of 15 mA/cm². (a) Capacitance vs. cycle number. (b) Coulombic efficiency vs. cycle number.

Fig. 8 is cycle charge–discharge test of the asymmetric supercapacitor at a current density of 15 mA/cm². The variation of the capacitance of the asymmetric supercapacitor was illustrated in Fig. 8a. As shown in Fig. 8a, capacitance of the supercapacitor reduced with the growth of cycle numbers. The capacitance value of initial (first cycle) is 46 F/g. After 1000 cycles, this value decreases to 41.5 F/g. The attenuation of the capacitance is about 10%. Fig. 8b suggests that the coulombic efficiency increased with the growth of cycle numbers.

4. Conclusion

In this study, RuO₂/TiO₂ nanotube composite was prepared by loading RuO₂ on TiO₂ nanotubes. The electrochemical test shows that the RuO₂/TiO₂ nanotube composite have electrochemical performance in the potential window from −0.4 to 0.4 V (versus Hg/HgO) and the AC within potential window (−1 to 0 V versus Hg/HgO) in KOH solution. An asymmetric supercapacitor based on RuO₂/TiO₂ nanotube composite and AC exhibits good electrochemical capacitance performance within potential range from 0 to 1.4 V. It shows a higher working voltage than a symmetrical supercapacitor based on RuO₂/TiO₂ nanotube composite as both negative and positive electrodes (a potential range of 0–0.8 V), leads to a high energy density, even there were no big capacitance differences between the asymmetrical supercapacitor and symmetrical supercapacitor. The energy density reached 12.5 Wh/kg at a power density of 150 W/kg and the energy density decreased to 5.7 Wh/kg when the power density increased up to 1207 W/kg. The supercapacitor also exhibits a good cycling performance and keep 90% of initial capacity over 1000 cycles.

Acknowledgements

Financial supports from 863 program of China (No. 2003AA32302) and the nano-project of Shanghai Nanotechnology Promotion Center (No. 0352 nm038) are acknowledged.

References

- [1] A. Rudge, J. Davey, I. Raistrick, S. Gottesfeld, *J. Power Sources* 47 (1994) 89.
- [2] A. Clemente, S. Panero, E. Spila, B. Scrosati, *Solid State Ionic* 85 (1996) 273.
- [3] C. Arbibzani, M. Mastragostino, L. Meneghello, R. Paraventi, *Adv. Mater.* 8 (4) (1996) 331.
- [4] M. Ishikawa, M. Morita, M. Ihara, Y. Matsuda, *J. Electrochem. Soc.* 141 (1994) 1730.
- [5] S.T. Mayer, Pekala, R.W. Pekala, J.L. Kaschmitter, *J. Electrochem. Soc.* 140 (1993) 446.
- [6] A. Rudge, J. Davey, I. Raistrick, S. Gottesfeld, *J. Power Sources* 47 (1994) 89.
- [7] A. Rudge, J. Davey, I. Raistrick, S. Gottesfeld, *Electrochim. Acta* 37 (1994) 273.
- [8] J.P. Zheng, T.R. Jow, *J. Electrochem. Soc.* 142 (1995) 6.
- [9] J.P. Zheng, P.J. Cygan, T.R. Jow, *J. Electrochem. Soc.* 142 (1995) 2699.
- [10] J.H. Park, O.O. Park, *J. Power Sources* 111 (2002) 185.
- [11] C. Arbizzani, M. Mastragostino, F. Soavi, *J. Power Sources* 100 (2001) 164.
- [12] A.D. Pasquier, I. Plitz, J. Gural, S. Menocal, G. Amatucci, *J. Power Sources* 113 (2003) 62.
- [13] A.D. Pasquier, A. Laforgue, P. Simon, *J. Power Sources* 125 (2004) 95.
- [14] T. Brousse, M. Toupin, D. Belanger, *J. Electrochem. Soc.* 151 (2004) 614.
- [15] Y.G. Wang, X.G. Zhang, *Electrochim. Acta* 49 (12) (2004) 1957.
- [16] Y.G. Wang, X.G. Zhang, *J. Electrochem. Soc.* 152 (4) (2005) 671.
- [17] X.M. Sun, Y.D. Li, *Chem. Eur. J.* 9 (2003) 2229.
- [18] B.E. Conway, *Electrochemical Supercapacitors*, Kluwer Academic/Plenum Publishers, New York, 1999.